frontiers | Frontiers in Ecology and Evolution

TYPE Original Research
PUBLISHED 15 May 2023
DOI 10.3389/fevo.2023.1166239

OPEN ACCESS

EDITED BY
Ahmed M. Eldosouky,
Suez University, Egypt

REVIEWED BY
Sherif Abu El-Magd,
Suez University, Egypt
Hadi Karimi,
Western Michigan University, United States

*CORRESPONDENCE
Guisheng Hu
✉ huguisheng@imde.ac.cn
Zhiquan Yang
✉ yzq1983816@kust.edu.cn

RECEIVED 15 February 2023
ACCEPTED 17 April 2023
PUBLISHED 15 May 2023

CITATION
He N, Song Y, Hu G, Yang Z, Fu Q and Gurkalo F (2023) The distribution law and coupling factors of debris flows in the G318 Linzhi–Lhasa section of the Sichuan–Tibet traffic corridor. *Front. Ecol. Evol.* 11:1166239. doi: 10.3389/fevo.2023.1166239

The distribution law and coupling factors of debris flows in the G318 Linzhi–Lhasa section of the Sichuan–Tibet traffic corridor

Na He[1,2], Yabing Song[2,3], Guisheng Hu[1]*, Zhiquan Yang[4,5,6]*, Qixuan Fu[2] and Filip Gurkalo[2]

[1]Institute of Mountain Hazards and Environment, Chinese Academy of Sciences, Chengdu, China, [2]School of Civil Engineering, Henan Polytechnic University, Jiaozuo, Henan, China, [3]China Jikan Research Institute of Engineering Investigation and Design, Co., Ltd., Xi'an, China, [4]Faculty of Public Safety and Emergency Management, Kunming University of Science and Technology, Kunming, Yunnan, China, [5]Key Laboratory of Geological Disaster Risk Prevention and Control and Emergency Disaster Reduction of Ministry of Emergency Management of the People's Republic of China, Kunming University of Science and Technology, Kunming, Yunnan, China, [6]Key Laboratory of Early Rapid Identification, Prevention and Control of Geological Disasters in Traffic Corridor of High Intensity Earthquake Mountainous Area of Yunnan Province, Kunming University of Science and Technology, Kunming, Yunnan, China

In recent years, debris flow disasters have occurred frequently along the highway, causing river blockages and road interruptions, which seriously threaten the safety of people's lives and property. Highway G318 is an important throat project linking Sichuan and Tibet; at the same time, it is an important channel for the economic development of Sichuan and Tibet and the transportation of national defense materials. Taking the Linzhi–Lhasa Section of Highway G318 as an example, this study analyses the distribution law and characteristics of coupling factors of debris flows in the study area (under its topographical, hydrometeorological, geological, and structural conditions) using remote sensing interpretation, field surveys, and mathematical statistics. The research shows that: (1) The types and quantity of debris flows in the region show statistical laws under the factors of the slope, slope aspect, drainage area, and gradient of the gully. The vegetation coverage in the upper reaches of the Nyang River valley gradually decreases, and the average debris flow disaster density is 0.529/km, which is the most densely distributed area of debris flow. (2) The distribution density of regional debris flows in narrow valleys is greater than that in wide valleys, and those in the Nyang River basin are greater than those in the Lhasa River basin. (3) By comparing the tectonic geological map and the debris flow distribution map, it was found that the debris flow distribution is controlled by faults, and 71% of the debris flow basins have faults. (4) There is a significant positive correlation between the gradient of the material source area and the gradient of the debris flow gully, as well as a close positive correlation between the rainfall and the fault density, and a close negative correlation between the average gradient and the drainage area. Due to the unique topography and geomorphology of different regions, a difference in meteorology and hydrology occurred. This further affected the topography, geomorphology, and distribution of debris flow disasters. Based on the study of the distribution law of regional debris flow and geological environmental factors, this study provides strong support for regional debris flow prevention and related research.

KEYWORDS

debris flow, distribution law, coupling factors, debris flow density, fault density

1. Introduction

The Sichuan–Tibet Highway is the most important land route from Sichuan to Tibet, passing through three major mountain ranges (the Hengduan Mountains, Nyainqentanglha Mountains, and the Himalayas) and four major water systems (the Yangtze River tributaries, Lancang River, Nujiang River, and Yarlung Zangbo River) (Lu and Cai, 2019; Yang et al., 2023a). The region is being squeezed by the Eurasian plate, with obvious mountain uplift and valley undercutting. The complicated geological tectonic movements have formed unique topography and climatic conditions, which makes the terrain gap of the Sichuan–Tibet Highway large, the regional climate difference obvious, and debris flow disasters frequently occur. Taking Peilonggou and Guxianggou as examples, the debris flow in Peilonggou was formed by ice avalanches. After blocking the Palong Zangbu River many times, the river weir dam was formed. After the dam broke, great harm was caused. As a result of massive debris flows in 1984 and 1985, the weir dam was formed and flooded 7 km upstream of the Sichuan–Tibet Highway, causing 79 vehicles to be destroyed. After the dam broke, 2 km of the downstream road and bridge were destroyed; several people died, and the economic loss was estimated at over 100 million yuan (Shang et al., 2003; Cheng and Wu, 2011; Zou et al., 2018; Emery et al., 2019; Chen et al., 2020; Liu et al., 2023; Yang et al., 2023b). The Guxianggou first broke out in 1953, with a huge viscous debris flow caused by the gully being blocked by the natural weir dam, formed by the accumulation of loose materials and landslide collapse caused by the Chayu earthquake (with a magnitude of 8.5) in 1950. Furthermore, due to the interaction between a rainstorm and high temperatures, the debris flow broke out, causing a large number of casualties and property damage. In the following years, several debris flows broke out, causing a huge loss of life and property. In 1953, a huge viscous glacial debris flow broke out in Guxianggou, causing more than 140 deaths and destroying a large number of highway subgrades, bridges, and cultivated lands (Zeng et al., 2007; Zou et al., 2018; Cui et al., 2022; Yang et al., 2023a). Large-scale viscous mud rock flows broke out in Tianmogou many times (e.g., in September 2007, July 2010, and September 2010), blocking the Palong Zangbu River many times, forming a barrier lake, and then, the G318 subgrade and bridge were destroyed after the breach (Wei et al., 2018). In September 2016, the Bitonggou, Chidan Nongbagou, and Jiaolonggou (in the Guxiang section of the Palong Zangbu basin) simultaneously broke out as a debris flow, silting up G318 and damaging the construction camp (Rappengluck, 2022).

There has been a large amount of research conducted by Chinese scholars as a result of a large number of debris flows along the Sichuan–Tibet Highway. Chen Hongkai analyzed the disaster-prone environment and formation mechanism of debris flow in the Sichuan section of the Sichuan–Tibet Highway through field investigations. The formation mechanism of a debris flow along the highway can be summarized into four categories: rainfall impact mechanism, intensity attenuation mechanism, scour cutting mechanism, and gully bed dragging mechanism (Shi et al., 2021; Zhao et al., 2023). Ye Tangjin used information entropy and FLAC numerical simulation to analyze the influencing factors of debris stability and the correlation of slope stability in the eastern part of the Sichuan–Tibet Highway. They established a debris slope stability evaluation model based on a support vector machine (Shang et al., 2003). Liu Xin studied the development environment, distribution characteristics, and laws of debris flow in the Bangda–Linzhi section of the Sichuan–Tibet Highway through field investigations and remote sensing. Previous studies revealed that topography, tectonic movement, stratigraphic lithology, and rainfall affect the scale and distribution of debris flows (Ye et al., 2022). Yuan Guangxiang, He Yiping, Jiang Zhongxin, and Zeng Qingli studied the characteristics of debris flow in the Palong Zangbo River Basin of the Sichuan–Tibet Highway. Yuan Guangxiang counted and classified the debris flow gullies along this section and analyzed the distribution law of debris flows. He Yiping believed that the debris flow source in this section is Quaternary deposits (debris flow deposits, landslide deposits, and avalanche deposits). The differential distribution law of landslides and debris flows was revealed by Jiang Zhongxin using quantitative methods, such as optimal segmentation and variance of ordered samples. Zeng Qingli thought that the geomorphological features of water systems are related to the development of debris flow groups and revealed the disaster mode of super-large debris flows (Shang et al., 2005; Kaczmarek and Popielski, 2019; Gao et al., 2021; Tang et al., 2022). Qi Yunlong put forward two kinds of action mechanisms at Jiuronggou, in the Bomi section of the Sichuan–Tibet Highway, affected by the combination of precipitation and temperature when debris flow starts (Zhou et al., 2014). Sun Yan used ETM+, Quickbird, and 30 m DEM (digital elevation model) data to interpret the geological disasters in the section of Highway G318 from Lhasa to Shigatse, by remote sensing via man–machine interaction (Xie et al., 2021).

As the main part of the Sichuan–Tibet Highway, Highway G318 is an important channel for Sichuan and Tibet's economic development and the transportation of national defense materials. The Linzhi–Lhasa section is characterized by undulating terrain, an elevation difference of about 2,000 m, and abundant rainfall; as a result, the disaster types in the study area are more diverse (Shen et al., 2019). However, there is little research on debris flow disasters in this section. Therefore, this study takes the Linzhi–Lhasa section as an example, based on detailed investigations, and uses ArcGIS and satellite images to extract statistical natural geological conditions. To explore the distribution law of debris flow under topography and geomorphology (slope of source area, slope direction, watershed area, gulf–bed ratio, and vegetation coverage rate), hydrometeorology (temperature and rainfall), and tectonic movement (fault), the correlation analysis method was used to discuss the distribution law of debris flow disasters under the coupling effect of factors such as slope, slope direction, watershed area, gully bed ratio, vegetation coverage, rainfall, and fault density and judge the main factors controlling the development of debris flow disasters. The aim is to provide a reference for disaster prevention and reduction in the operation and maintenance of this section of the highway.

2. Study area profile

2.1. Topographic and geomorphic conditions

The study area is located in the suture zone between the Eurasian plate and the Indian Ocean plate, which is surrounded by mountains: the Nyainqentanglha Mountain in the west, the eastern Himalayan Mountains in the south, and the Hengduan Mountains in the east.

The Linzhi–Lhasa section of Highway G318 starts from Linzhi Town in the east and ends in Lhasa in the west, passing through the Bayi District, Gongbujiangda County, and Mozhugongka County, with a total length of 420 km (Figure 1). The terrain is undulating, from Milla Mountain (elevated to about 5,000 m) to the Bayi District (elevation 2,900 m), passing through the source of the Nyang River and the Lhasa River. The valley in the Nyang River basin narrows from wide to narrow (upstream), while the valley in the Lhasa River basin is relatively wide (downstream). With the increase in altitude, the vegetation is less, the external forces are strong, and the rock mass is severely weathered. The loose deposits on Milla Mountain are mainly sand slopes, and some of them contain moraines. On the left-hand side of Milla is the Linzhi section, which has good vegetation and abundant rainfall. On the right-hand side is the Lhasa section, with little vegetation coverage (mainly alpine meadows) and rich material sources in ditches and bank slopes (Figure 2).

2.2. Geological conditions

The study area is located in the Lhasa–Bomi fold belt, which is an east–west structural system; it is the east wing of the Pamir–Himalayan structure. Its structural features are a series of nearly east–west faults and folds, and the structural unit belongs to the Gangdise–Tengchong micro-land block. Under neotectonic movement, there is a strong vertical uplift and horizontal sliding of the block (Mikos, 2011; Zhang et al., 2011; He et al., 2022). Under this complex geological activity and structure, the regional seismic activity is relatively strong. The area is located in the seismic belt of central Tibet, with a peak acceleration of ground motion of 0.1∼0.3 g ($g = 9.8 m/s^2$), a characteristic period of ground motion response spectrum of 0.45 s, and an upper limit of potential earthquake source magnitude of 6.9 (Figure 3).

2.3. Hydrometeorological conditions

The study area is located in an area of strong and uplifted neotectonic movement. The climate in the area is complicated and changeable due to the influence of the Himalayan Mountains, Nyainqentanglha Mountains, and Hengduan Mountains. The Nyang River and Lhasa River are well-developed in the area. The Nyang River originates from Milla Mountain and joins the Yarlung Zangbo River in the Bayi District. The Lhasa River originates at the southern foot of Nyainqentanglha Mountain, passes through Lhasa, and finally joins the Yarlung Zangbo River. The climate of the Linzhi section on the left-hand side of Milla is formed by the convergence of hot and humid Indian Ocean airflow along the Yarlung Zangbo River and dry and cold continental airflow, which forms the unique climatic conditions of Linzhi. It is warm and rainy in the summer. The annual rainfall in most areas ranges from about 600 mm to 1,000 mm; the snow line elevation is between 4,500 m and 4,700 m; and the annual rainfall can reach 2,500 to 3,000 mm (Zhang et al., 2011). The temperature difference is large, and the ice and snowmelt are serious (Paul, 2019; Jia et al., 2020; Zeng et al., 2023). The winter is dry and cold, and the climate is slightly different at higher elevations. The climate of the Lhasa section on the right-hand side of Milla is mainly controlled by the semi-arid monsoon climate in the temperate zone of the plateau. The annual average rainfall is about 200–510 mm, mainly concentrated from June to September (Ma et al., 2021), and the vegetation is scarce, mainly comprising alpine meadows.

According to the data statistics of the meteorological stations in the study area (Bayi Station and Mozhugongka Station in Figures 4, 5, respectively) from the last 30 years (1992–2021), the regional rainfall distribution law can be analyzed. The annual average temperature of Bayi Station is 9.2°C; the average temperature of the coldest month (January) is 1.2°C, and the average temperature of the hottest month (July) is 16.4°C. The extreme maximum temperature is 31.4°C, and the extreme minimum temperature is −13.6°C. The average annual precipitation is 690.5 mm, and the precipitation from March to October accounts for about 98.4% of the whole year; the precipitation from November to February only accounts for 1.6% of the whole year. The annual relative humidity is 66%. The annual average temperature in the urban area of Mozhugongka County is 6.7°C; the average temperature in the coldest month (January) is −2.55°C, and the average temperature in the hottest month (June) is 14.3°C; the extreme maximum temperature is 53°C; the average annual precipitation is 583.4 mm, and the precipitation from March to October accounts for about 98.5% of the whole year; the precipitation from November to February only accounts for 1.5% of the whole year.

3. Methods and data sources

Temperature and rainfall, formation lithology, geological structure, and fault distribution in the study area were identified based on the collected meteorological, hydrological, and geological environment data. According to the characteristics of the debris flow basin, 119 debris flow gullies were identified along Highway G318 using remote sensing images. Through field investigations (supplemented and verified by the results of remote sensing), it was found that there are 164 debris flow gullies in the area, of which the distribution of debris flow along G318 is shown in Figure 6.

According to China's Second Glacier Catalog, the glaciers in the study area cover an area of 1560.86 km^2, accounting for 6% of the study area. The glaciers are primarily distributed at the source area of high-altitude valleys in the middle and lower reaches of the Nyang River, and the largest distribution in the Zhulaqu basin is located in the middle reaches of the Nyang River (including 42 debris flow ditches created by glaciers). Glacier meltwater is one of the water source conditions (Figure 2). Remote sensing interpretation and satellite images show 36 glacial lakes in the

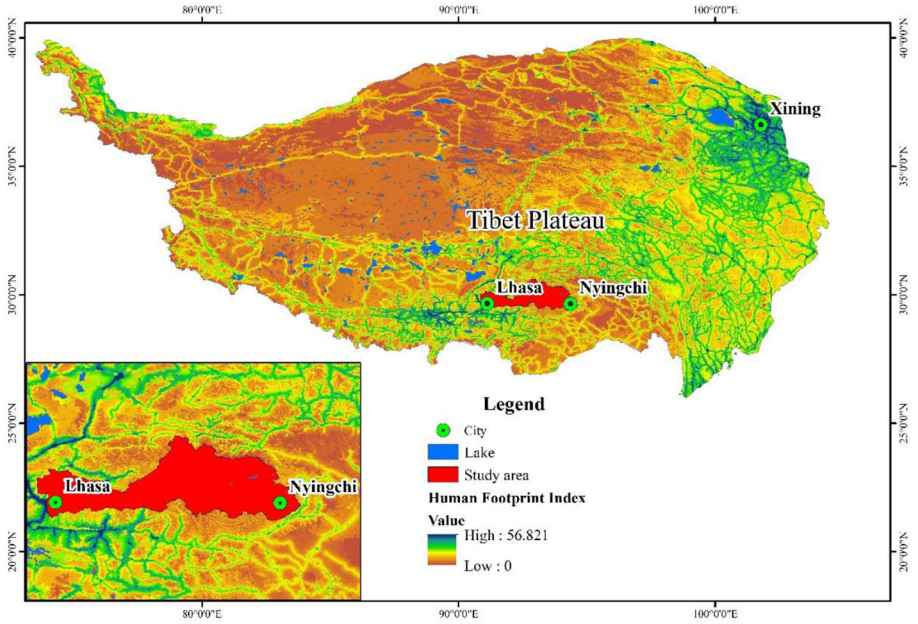

FIGURE 1
Geographical location map of the study area.

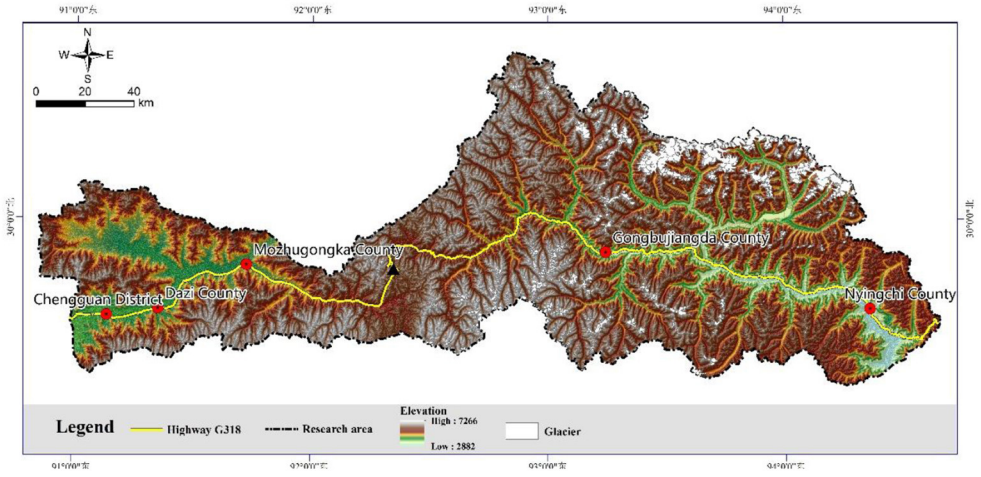

FIGURE 2
Rendering map of topography and geomorphology and section location map.

debris flow basin. The largest area of a single glacial lake is 0.55 km^2, and those smaller than 0.1 km^2 are less likely to cause debris flow. The debris flow basin in the statistics area contains 11 glacial lakes with an area larger than 0.1 km^2, which may trigger debris flow due to the influences of glacial lake outbursts. In the study area, the altitude is high and the terrain fluctuates greatly. The perennial glaciers and seasonal snowmelt become one of the water sources of debris flow. According to the distribution of temperature, precipitation, glaciers, and seasonal snow and ice, the debris flow is classified according to the water source conditions of the debris flow, with Milla Mountain as the boundary (Table 1).

First, based on ASTER GDEM 30 m elevation data and ArcGIS spatial analysis platform, data such as boundary, gully elevation, topographic relief, slope, and slope direction of the study area are extracted. Second, the normalized index NDVI was synthesized using Landsat 8-9 OLI/TIRS C2 L2 remote sensing data. Finally, the geological map of the study area was registered, and the measured faults were vectorized to analyze the spatial distribution of debris flows under various factors. In order to explore the disaster environment of debris flow, Pearson's linear correlation and Spearman's correlation analysis are used to analyzing the correlation characteristics of gully slope degree, slope direction,

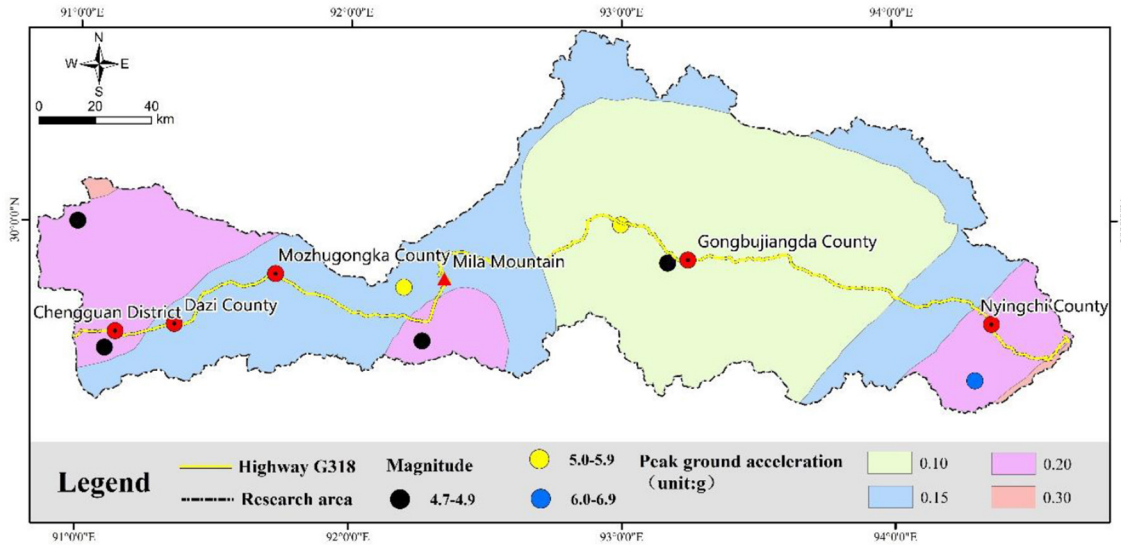

FIGURE 3
Peak acceleration and epicenter distribution of earthquakes.

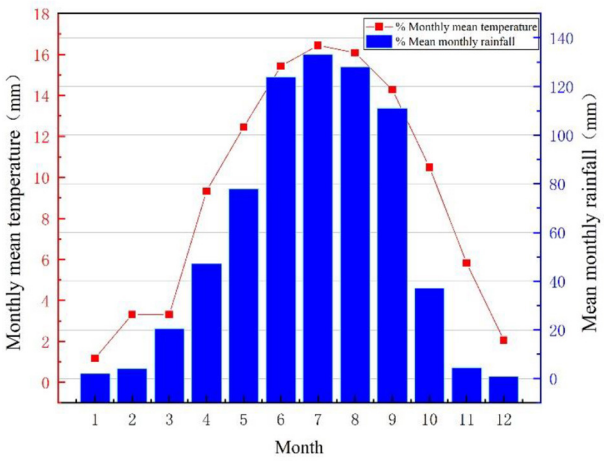

FIGURE 4
Average annual temperature and rainfall in Bayi Station from 1992 to 2021.

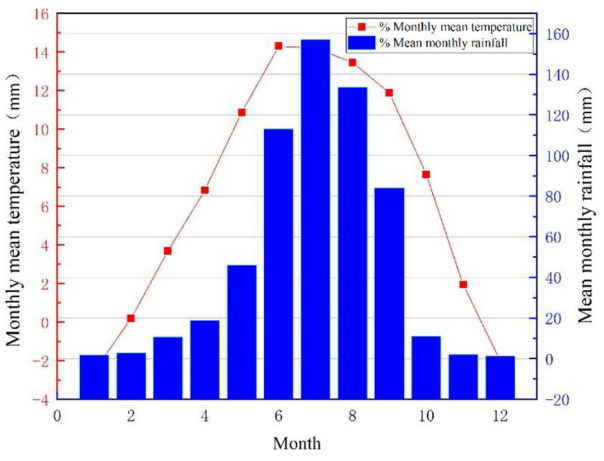

FIGURE 5
Average annual temperature and rainfall in Mozhugongka Station from 1992 to 2021.

basin area, gully bed ratio, vegetation coverage, rainfall, and fault density in the debris flow basin.

3.1. Distribution of debris flow along G318

As a result of a combination of internal and external forces, debris flow gullies are formed. Under the action of internal forces, plates drift, squeeze, and separate to form mountain valleys, which determine the location, elevation, distribution, and source of faults and solid loose materials in the debris flow gully. Under the action of external forces, temperature, and rainfall affect the area of the debris flow basin, the weathering degree of solid materials, and the change in topography in the area.

Located in the Himalayan tectonic region, the study area is squeezed between the Indian Ocean plate and the Eurasian plate. The climate is jointly controlled by continental cold and dry air flow and hot and humid air flow from the Indian Ocean. There are all types of debris flow disasters in the area. According to the field survey, combined with the regional characteristics, the debris flow distribution is bounded by Milla Mountain. The average disaster density along G318 in the east of Milla Mountain is 0.490/km, and the average disaster density in the west of Milla Mountain is 0.275/km.

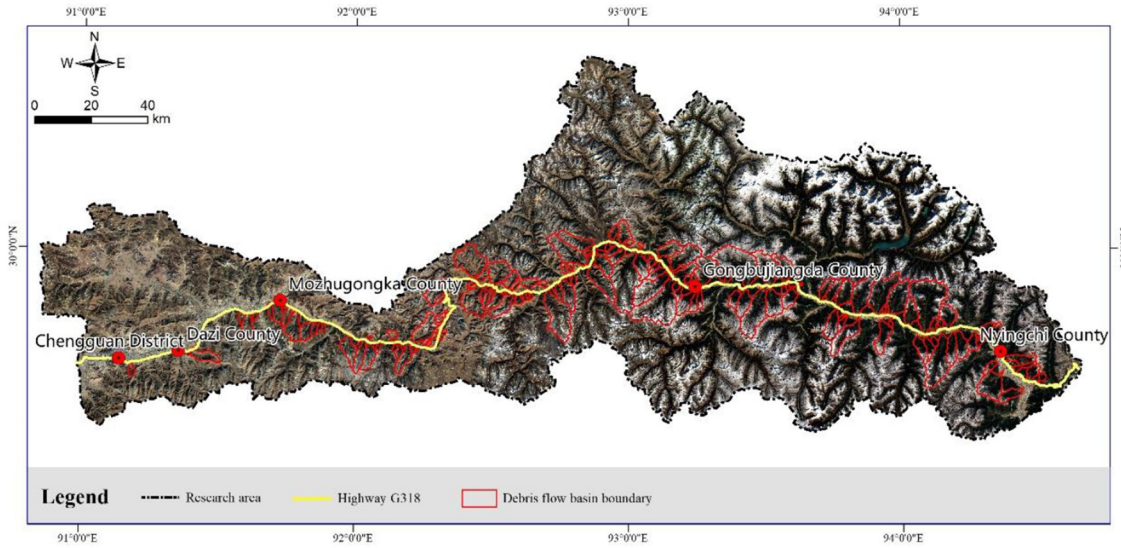

FIGURE 6
Satellite images and debris flow distribution.

TABLE 1 Classification of debris flow types in the study area.

Type	Rainfall-induced debris flow (number)	Glacial meltwater debris flow (rainfall-induced and glacial meltwater) (number)	Mixed debris flow (rainfall-induced, glacial meltwater and glacial lake burst) (number)
East of Milla	88	27	8
West of Milla	34	4	3

3.2. Distribution characteristics of debris flow under topographic conditions

3.2.1. Gradient of debris flow source area

The gradient of the source area directly affects the scale of debris flow and the mode and quantity of solid material supply (Cui et al., 2022). ArcGIS was used to extract the gradient of the source area of 164 debris flow gullies in the study area; mathematical statistics were then used to analyze the differential distribution rule of the gradient of debris flow gullies in the source area (Figure 7A). The number of debris flow gullies with a gradient of $<30^{\circ}$ in the source area accounts for 79%, and the number of rainfall-induced, glacial meltwater, and mixed debris flow gullies (rainfall-induced, glacial meltwater, and glacial lake break-caused debris flow gullies) accounts for 91% of non-rainfall-induced debris flow gullies. This indicates that the main mode of supply for the debris flow sources in the area is landslides with a relatively gentle slope and loose solid materials accumulating in valleys. The main types of debris flow source areas with a relatively larger gradient are debris flow deposits, sand slide deposits, landslide deposits, collapse, etc. In addition, the gradient of the source areas of debris flows associated with glacial meltwater and glacial lake outbursts is generally small.

3.2.2. Slope aspect of the material source area

The slope aspect has a significant influence on the formation, distribution, and activity intensity of debris flow (Cui et al., 2022). North-facing slopes in the northern hemisphere (shady slopes) have the least sunshine hours and solar radiation intensity, which is conducive to the accumulation and storage of snow and ice. The south-facing slopes (sunny slopes) have the most sunshine hours and higher solar radiation intensity, which is conducive to creating meltwater from ice and snow glaciers and stratum weathering; they are prone to debris flows. According to the statistics of the slope aspect of 164 debris flow gullies in the formation area, the analysis shows that most of the debris flow gullies on the north slope (0.0–22.5° and 337.5–360.0°) are rainfall-induced, and the probability of glacier meltwater and ice lake outburst-caused debris flows is low, accounting for 16% of the debris flow gullies on the north slope and 12% of the non-rainfall-induced debris flows. From the east slope to the south slope (45–225°), the probability of glacier meltwater and ice lake outburst-caused debris flow is high, accounting for 53% of non-rainfall-induced debris flow (Figure 7B).

3.2.3. Drainage area

The differential distribution characteristics of debris flow gullies under different drainage areas were analyzed according to the drainage area statistics of 164 debris flow gullies in the study area (Figure 7C). The analysis shows that about 13% of the debris flow gullies have a drainage area of <2 km^2, about 15% of the debris flow gullies have a drainage area of more than 100 km^2, and about 72% of the debris flow gullies have a drainage area of 2–100 km^2. The number of debris flow gullies increases at first but then decreases, with a gradual increase in the drainage area. About

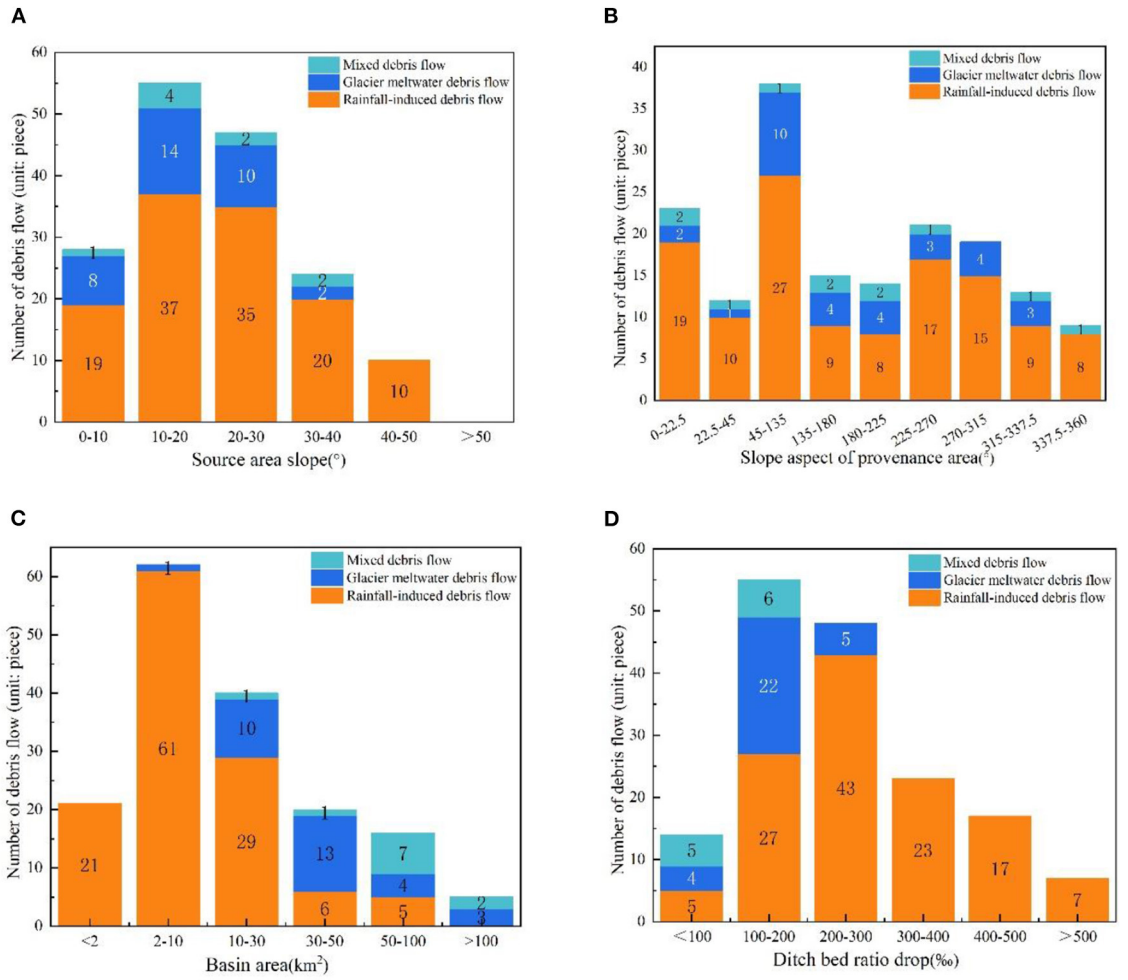

FIGURE 7
Distribution characteristics of debris flow gullies under different topography conditions. **(A)** The relationship between debris flow initiation and slope of the source area. **(B)** The relationship between debris flow initiation and slope aspect of the provenance area. **(C)** The relationship between debris flow initiation and drainage area. **(D)** The relationship between debris flow initiation and gradient of debris flow gullies.

91% of the rainfall-induced debris flows have a drainage area of <30 km^2, and the glacial meltwater debris flows and glacial lake outburst debris flows have a drainage area of more than 10 km^2. This indicates that the rainfall-induced debris flows mostly occur in the gullies with smaller drainage areas, while the glacial meltwater debris flows and glacial lake outburst debris flows have larger drainage areas.

3.2.4. Gradient of debris flow gullies

The gradient of a gully is the bottom-bed condition for fluid to change from potential energy to kinetic energy, and it is an important condition that affects the formation and movement of debris flow (Cui et al., 2022). The greater the gradient of a debris flow gully, the greater the potential energy conditions for the debris flow, which facilitates its initiation. The statistical analysis of the gradient of the 164 debris flow gullies in the study area established the relationship between the gradient and its distribution (Figure 7D). The analysis shows that ~9% of debris flows have ditch bed ratio drops <100‰, ~7% of debris flows have ditch bed ratio drops more than 500, and 87% of debris flows have ditch bed ratio drops between 100 and 500‰. The debris flow gully gradually increases and then decreases with increasing gradient, similar to the distribution characteristics of the debris flow gully under the drainage area. The reason for this is that the debris flow gully gradient has a linear relationship with the drainage area. Approximately 88% of glacial meltwater and glacial lake outburst-caused debris flows have gully gradients <200‰ and ~74% of rainfall-induced debris flows have gully gradients >200‰. Generally, glacial meltwater and mixed debris flows have smaller gully gradients, while rainfall-induced debris flows have larger gully gradients.

3.2.5. Vegetation coverage (NDVI: normalized difference vegetation index)

Surface vegetation coverage affects the occurrence and development of geological disasters. Trees and shrubs with high vegetation coverage and well-developed roots have strong soil and water conservation abilities, and the frequency of geological disasters caused by precipitation is extremely low (Lara and Sepulveda, 2010). The analysis shows that the valley vegetation

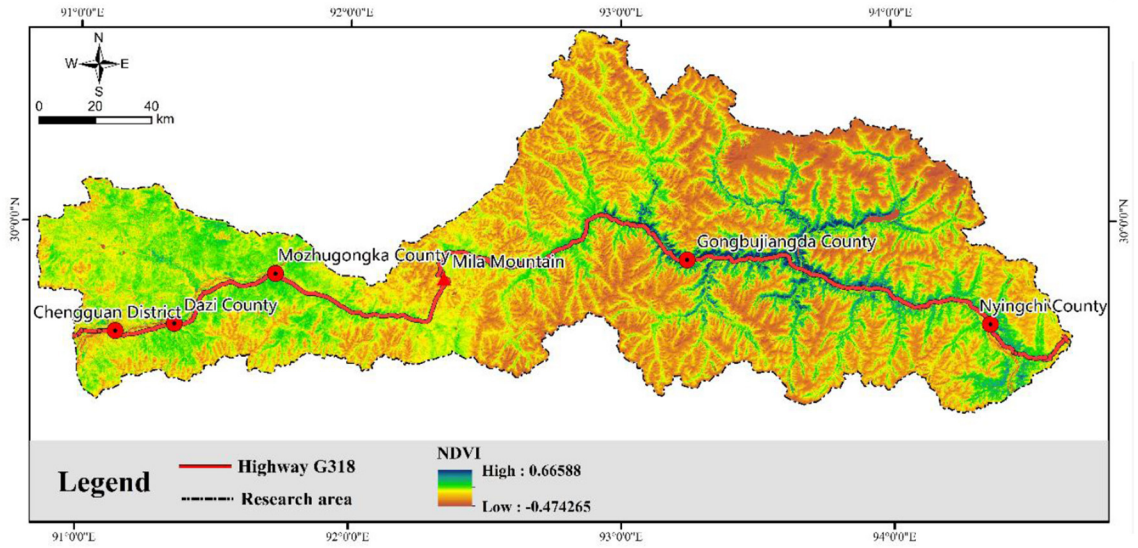

FIGURE 8
Vegetation coverage of the study area.

coverage is high in the middle and lower reaches of the Nyang River in the study area (Figure 8). The top of the mountain is covered with snow and glaciers all year round, with low vegetation coverage. The average density of the debris flow is 0.426/km, and the distribution is relatively dense. The vegetation coverage of the valley in the upper reaches of the Nyang River has gradually been reduced, the weathering and erosion of rocks on the mountain slope are strong, the rocks in the valley have piled up, and the average density of debris flow is 0.529 /km, which is the most densely distributed area of debris flow. The vegetation in the Lhasa River basin is generally an alpine meadow, with gentle terrain and low distribution of debris flow.

3.3. Distribution characteristics of debris flow under different hydrometeorological conditions

Regional topography affects regional hydrometeorology, and hydrometeorology reshapes topography. The unique topographic and geomorphological conditions in the study area make temperature and precipitation change significantly, which leads to obvious differences in surface vegetation coverage, weathering, and denudation of the rock mass, the water source, and the material source of debris flow. Both temperature and rainfall have important influences on the development and distribution of debris flows.

Mozhu Maqu, a tributary of the Lhasa River and Nyang River, originates from glacial meltwater and widens along the river valley. The rainfall in the Nyang River basin is abundant, while that in the Lhasa River basin is small. According to the change in valley topography, the study selects nodes to draw the river's geological section. The locations of the sections are shown in Figure 2. As a result of the analysis, topography complexity can be summarized as follows: 2-2 section > 1-1 section > 3-3 section > 4-4 section (Figure 9). According to the change in the valley landform and the difference in temperature and rainfall conditions, the area is divided into four parts: cross-section 1-1 to cross-section 2-2 (wide section of the Nyang River), cross-section 2-2 to Milla Mountain (narrow valley cross-section of the Nyang River), Milla to cross-section 3-3 (narrow valley section of Mozhu Maqu), and cross-section 3-3 to cross-section 4-4 (wide valley cross-section of the Lhasa River) (Figure 2). A combination of highway debris flow distribution characteristics and the disaster density indicates that the regional debris flow distribution density from section 2-2 to Milla Mountain (0.528/km) > from section 1-1 to section 2-2 (0.429/km) > from Milla Mountain to section 3-3 (0.417/km) > from section 3-3 to section 4-4 (0.136/km). This means that the regional debris flow distribution density in the narrow valley section is greater than that in the wide part, and the Nyang River basin (with large rainfall) is greater than that in the Lhasa River basin (with less rainfall).

3.4. Distribution characteristics of debris flow under the influences of geological tectonic activities

Under the compression of the Indian Ocean and Eurasian plates, the Qinghai-Tibet Plateau rises as a whole, ignoring the influence of local stratum uplift and the reduced distribution of regional debris flows. In the study area, faults are mostly developed in an east–west direction. Several faults per unit area (fault density) were used to analyze debris flow distribution (Figure 10). The faults in this area are concentrated in the Nyang River basin, and the north bank has more faults than the south bank. About 71% of debris flow gullies are affected by faults, with fault strikes generally perpendicular to the debris flow gullies. The density and distribution of faults show that, in areas with strong geological tectonic action (the east side of Milla and the north bank of the

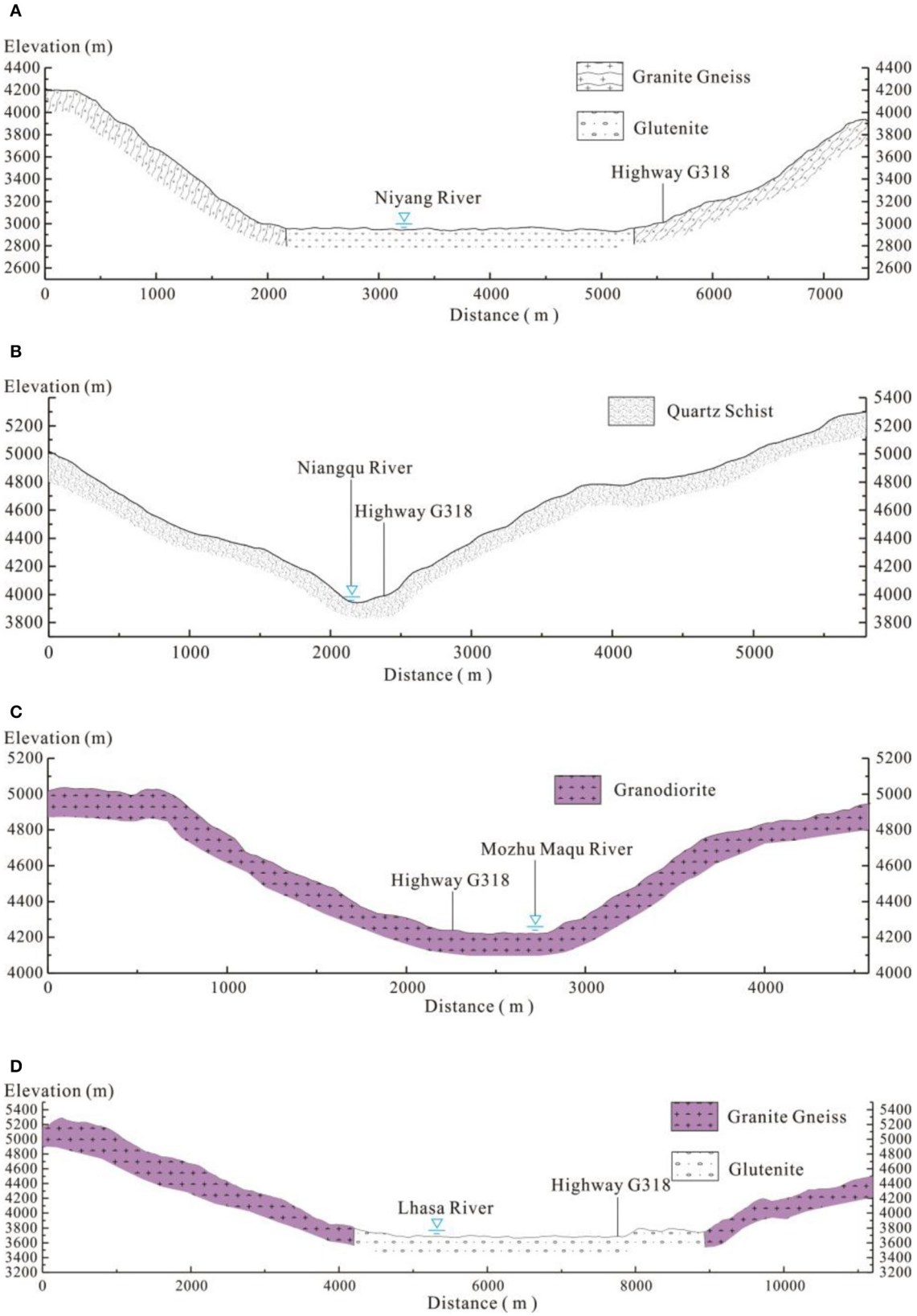

FIGURE 9
Characteristics of the cross-sections in the main river. **(A)** 1-1 Cross-section in the lower reaches of the Niyang River. **(B)** 2-2 Cross-section in the upper reaches of the Niyang River. **(C)** 3-3 Cross-section of Mozhu Maqu River. **(D)** 4-4 Cross-section of Lhasa River.

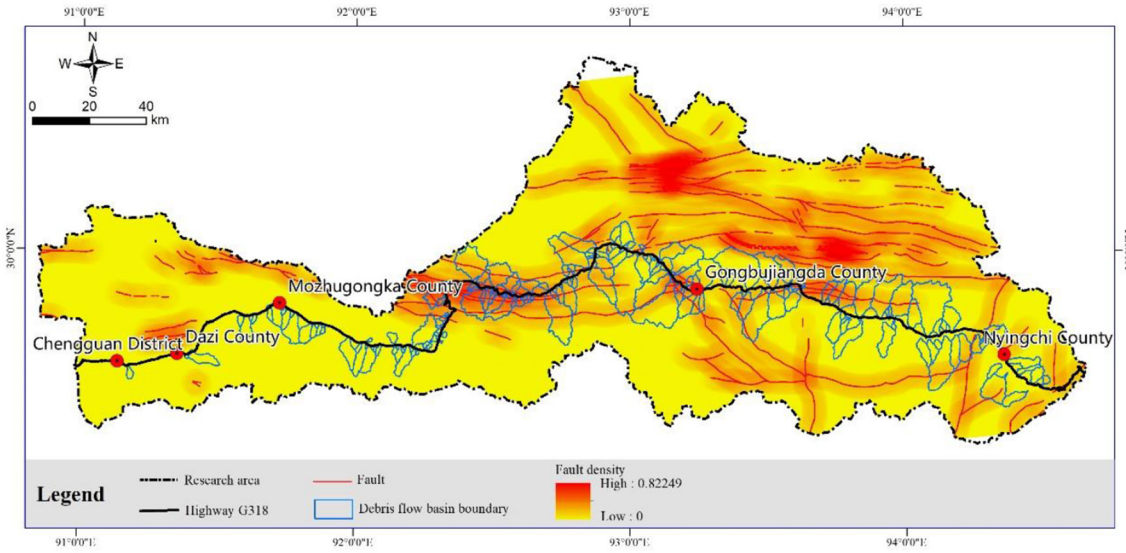

FIGURE 10
Faults and their density in the study area.

middle and lower reaches of the Nyang River), the rock mass structure is easily destroyed under the action of faults, forming numerous of broken rock masses and loose accumulations, which provide abundant materials for debris flow initiation. The degree of development of debris flow in the fault region is strong, and debris flow gullies are mostly distributed in areas with high fault density.

4. Discussion

The disaster-prone environment of debris flows arises from the coupling of natural and geological conditions, so analyzing the distribution of debris flows under a single factor seems very limited. The coupling effect of natural environmental factors determines debris flow development and distribution. Factors such as slope, slope aspect, drainage area, gully gradient, vegetation coverage, rainfall, and fault density in the debris flow watershed were selected. Pearson's and Spearman's correlation analysis (Chia, 1999) was used to evaluate the significance and analyze the correlation characteristics of each factor.

Pearson's correlation analysis must meet the following conditions: (a) Data are continuous variables and appear in pairs; (b) Data are normal. (c) Data are normally distributed. The slope, slope direction, drainage area, gully bed gradient, vegetation coverage, rainfall, and fault density of the study area all appear in pairs, among which rainfall and fault density are discontinuous variables. The box diagram can determine whether the sample data have outliers. If there are outliers, the mean value of the sample can be used to replace them. After analysis, the data from Nos. 21, 49, and 62 watersheds in the samples were abnormal, thus, the mean value of the data was used to replace the abnormal value in the analysis. By analyzing the gully bed gradient data, it was found that the data of Nos. 40, 42, and 70 watersheds were abnormal, and the mean value of the data was used in this study. Through the analysis of the descriptive statistics results,

TABLE 2 Pearson's correlation of coupling factors in disaster-prone environment of debris flow.

Coupling factor	Slope	Average gradient	Drainage area	Vegetation coverage
Slope	1.000	0.617**	−0.308**	0.305**
Average gradient	0.617**	1.000	−0.618**	0.387**
Drainage area	−0.308**	−0.618**	1.000	−0.272**
Vegetation coverage	0.305**	0.387**	−0.272**	1.000

**Indicates that it is at the level of 0.01 (two-tailed) and the correlation is significant.

TABLE 3 Spearman's correlation of coupling factors in the disaster-prone environment of debris flow.

Coupling factor	Rainfall	Slope aspect	Fault density
Rainfall	1.000	0.126	0.743**
Slope aspect	0.126	1.000	0.126
Fault density	0.743**	0.126	1.000

**Indicates that it is at the level of 0.01 (two-tailed) and the correlation is significant.

it can be seen that the slope direction does not obey a normal distribution. Therefore, Pearson's correlation analysis was used for slope, average gradient, vegetation coverage, and drainage area (Table 2). Spearman's correlation analysis is suitable for detecting variables with monotone relationships. The graph builder in the SPSS software is used to test the monotonicity of slope direction, rainfall, and fault density, and the test results show that the sample data have significant monotonicity, thus, slope direction, fault density, and rainfall are analyzed by Spearman's correlation analysis (Table 3). The measurement standard for correlation coefficients is shown in Table 4.

TABLE 4 Measurement standard of the correlation coefficient.

Degree of relationship	Positive correlation coefficient	Negative correlation coefficient
Very close	0.7∼1.0	−1.0∼−0.7
Close	0.4∼0.7	−0.7∼−0.4
General	0.2∼0.4	−0.4∼−0.2
Weak	0.0∼0.2	−0.2∼0.0

The study results indicate a strong positive correlation between slope and average gradient, a relatively negative correlation between slope and drainage area, and a relatively positive correlation between slope and vegetation coverage. Furthermore, there is a very strong positive correlation between rainfall and fault density. The average gradient has a close negative correlation with drainage area and an overall positive correlation with vegetation coverage. Moreover, there is a generally negative correlation between drainage area and vegetation coverage. The reason for this lies in the unique topography of the study area, which leads to regional differences in meteorology and hydrology. Regional differences in meteorology and hydrology reshape topography and geomorphology, coupling natural geological and environmental factors. As the regional terrain slope becomes more complex, the average gradient within debris flow basins increases, resulting in a smaller average gradient within the debris flow basin as the debris flow area increases. As a result of intensive geological activity and high fault density, regional elevations are raised, which blocks flow cases convection of airflow, resulting in variations in rainfall across the region. As the formation condition and excitation factor of debris flow, rainfall controls debris flow activity characteristics. Different rainfall patterns in different regions contribute to the spatial distribution differences of debris flows in the east and west of the study area and affect the development characteristics, frequency, and scale of debris flows.

5. Conclusion

In this study, field surveys, remote sensing interpretation, laboratory testing, and model calculations were used to study the distribution law and coupling factor characteristics of debris flow along Highway G318, from Linzhi to Lhasa, considering topography, meteorology, hydrology, and geological structure. The following conclusions are drawn:

(1) The main sources of debris flow in the study area are landslides with a gentle slope and loose deposits accumulated in gullies; the debris flow gullies on the north slope are mostly rainfall-induced debris flow; and the probability of glacial meltwater and glacial lake outburst debris flow is higher from the east slope to the south slope. The gradient of the debris flow gully is normally distributed. Generally, the gradient of a glacial meltwater and mixed debris flow gully is small, and the gradient of a rainfall-induced debris flow gully is large. The lower the vegetation coverage, the greater the debris flow gully density.

(2) The distribution density of debris flow in a narrow valley is greater than that in a wide valley, and the Nyang River basin (with large rainfall) is larger than the Lhasa River basin (with less rainfall).

(3) The degree of development of debris flow in the fault area is strong, and debris flow gullies are mostly distributed in areas with high fault density.

(4) The unique topography leads to regional meteorological and hydrological variations, which reshape the topography, resulting in a coupling effect between the natural and geological conditions. The regional terrain slope becomes more complex, and the average gradient of the debris flow basin becomes larger; the larger the debris flow area is, the smaller the average gradient is. A combination of intensive geological activities and relatively high fault density causes regional elevation rise, which blocks the flow and convection of airflow, leading to variations in rainfall patterns.

These research conclusions have important scientific value for the analysis of the cause of debris flow and the establishment of monitoring and warning in the later stage.

Data availability statement

The original contributions presented in the study are included in the article/supplementary material, further inquiries can be directed to the corresponding authors.

Author contributions

NH: writing, methodology, reviewing, and editing. YS and QF: data processing and writing. GH: original draft and data processing. GH and FG: reviewing and editing. ZY and QF: conceptualization and methodology. All authors contributed to the article and approved the submitted version.

Funding

This study was financially supported by the Second Comprehensive Scientific Investigation of Qinghai-Tibet Plateau (No. 2019QZKK0902), International (Regional) Cooperation and Exchange Project of National Natural Science Foundation of China: Occurrence Mechanism and Risk Control of Multi-scale Landslide and Debris Flow Disaster Chain (No. 41861134008), Project of Youth Innovation Promotion Association of Chinese Academy of Sciences (No. 2020367), the Muhammad Asif Khan academician workstation of Yunnan Province (Grant No. 202105AF150076), and the Key R&D Program of Yunnan Province (Grant No. 202003AC100002).

Conflict of interest

YS was employed by the China Jikan Research Institute of Engineering Investigation and Design, Co., Ltd.

The remaining authors declare that the research was conducted in the absence of any commercial or financial relationships that could be construed as a potential conflict of interest.

Publisher's note

References

Chen, Z. Q., He, C., Yang, W. B., Guo, W. Q., Li, Z., Xu, G. W., et al. (2020). Impacts of geological conditions on instability causes and mechanical behavior of large–scale tunnels: a case study from the Sichuan–Tibet highway, China. *Bull. Eng. Geol. Environ.* 79, 3667–3688. doi: 10.1007/s10064-020-01796-w

Cheng, Z. L., and Wu, J. S. (2011). "Formation of dam from debris flow in the southeast Tibet" in *The 8th cross-strait symposium on mountain disasters and environmental conservation* (Beijing: Chinese Society of Soil and Water Conservation), 39–45.

Chia, K. S. (1999). Multivariate statistical analysis: a brief introduction. *Ann Acad Med Singap*. 28, 879–880.

Cui, P., Ge, Y. G., Li, S. J., Li, Z. H., Xu, X. W., Zhou, G. G. D., et al. (2022). Scientific challenges in disaster risk reduction for the Sichuan–Tibet Railway. *Eng. Geology*309, 1–20. doi: 10.1016/j.enggeo.2022.106837

Emery, A. R., Hodgson, D. M., Barlow, N. L. M., Carrivick, J. L., Cotterill, C. J., Phillips, E., et al. (2019). Left high and dry: deglaciation of Dogger Bank, North Sea, recorded in proglacial lake evolution. *Front. Earth Sci.* 7, 234. doi: 10.3389/feart.2019.00234

Gao, R. Y., Wang, C. M., Liang, Z., Han, S. L., and Li, B. L. (2021). A research on susceptibility mapping of multiple geological hazards in Yanzi River Basin, China. *Int. J. Geo-Information* 10, 1–25. doi: 10.3390/ijgi10040218

He, N., Fu, Q. X., Zhong, W., Yang, Z. Q., Cai, X. Q., Xu, L. J., et al. (2022). Analysis of the formation mechanism of debris flows after earthquakes–A case study of the Legugou debris flow. *Front. Ecol. Evolution* 10, 1–17. doi: 10.3389/fevo.2022.1053687

Jia, X. L., Wang, D., Liu, F. B., and Dai, Q. M. (2020). Evaluation of highway construction impact on ecological environment of Qinghai-Tibet Plateau. *Environ. Eng. Manage. J.* 19, 1157–1166. doi: 10.30638/eemj.2020.109

Kaczmarek, L. D., and Popielski, P. (2019). Selected components of geological structures and numerical modelling of slope stability. *Open Geosciences* 11, 208–218. doi: 10.1515/geo-2019-0017

Lara, M., and Sepulveda, S. A. (2010). Landslide susceptibility and hazard assessment in San Ramn Ravine, Santiago de Chile, from an engineering geological approach. *Environ. Earth Sci.* 60, 1227–1243. doi: 10.1007/s12665-009-0264-5

Liu, Z. Q., Yang, Z. Q., Chen, M., Xu, H. H., and Yang, Y. (2023). Research hotspots and frontiers of mountain flood disaster: bibliometric and visual analysis. *Water* 15, 1–19. doi: 10.3390/w15040673

Lu, C. F., and Cai, C. X. (2019). Challenges and countermeasures for construction safety during the Sichuan–Tibet Railway project. *Engineering* 5, 833–838. doi: 10.1016/j.eng.2019.06.007

Ma, C., Li, T. T., and Liu, P. (2021). GIMMS NDVI3g+(1982-2015) response to climate change and engineering activities along the Qinghai–Tibet railway. *Ecol. Indic.* 128, 7821. doi: 10.1016/j.ecolind.2021.107821

Mikos, M. (2011). Public perception and stakeholder involvement in the crisis management of sediment-related disasters and their mitigation: the case of the Stoze debris flow in NW Slovenia. *Int. Environ. Assessment Manage.* 7, 216–227. doi: 10.1002/ieam.140

Paul, F. (2019). Repeat glacier collapses and surges in the Amney Machen mountain range, Tibet, possibly triggered by a developing rock-slope instability. *Remote Sensing* 11, 1–17. doi: 10.3390/rs11060708

Rappengluck, M. A. (2022). Natural iron silicides: a systematic review. *Minerals* 12, 2. doi: 10.3390/min12020188

Shang, Y. J., Park, H. D., and Yang, Z. F. (2005). Engineering geological zonation using interaction matrix of geological factors: an example from one section of Sichuan-Tibet Highway. *Geosci. J.* 9, 375–387. doi: 10.1007/BF02910326

Shang, Y. J., Yue, Z. Q., Yang, Z. F., Wang, Y. C., and Liu, D. A. (2003). Addressing severe slope failure hazards along Sichuan–Tibet Highway in Southwestern China. *Episodes* 26, 94–104. doi: 10.18814/epiiugs/2003/v26i2/003

Shen, T., Wang, Y. S., Luo, Y. H., Xin, C. C., Liu, Y., He, J. X., et al. (2019). Seismic response of cracking features in Jubao Mountain during the aftershocks of Jiuzhaigou Ms7.0 earthquake. *J. Mountain Sci.* 16, 2532–2547. doi: 10.1007/s11629-019-5570-0

Shi, X. G., Jiang, L. M., Jiang, H. J., Wang, X. D., and Xu, J. H. (2021). Geohazards analysis of the Litang–Batang section of Sichuan–Tibet Railway using SAR interferometry. *IEEE J. Appl. Observ. Remote Sensing* 14, 11998–12006. doi: 10.1109/JSTARS.2021.3129270

Tang, J. B., Liu, C., Mao, J. J., and Wang, H. (2022). Numerical simulation and hazard analysis of debris flows in Guxiang Gully, Tibet, China. *Front. Earth Sci.* 10, 16648714. doi: 10.3389/feart.2022.908078

Wei, R. Q., Zeng, Q. L., Davies, T., Yuan, G. X., Wang, K. Y., Xue, X. Y., et al. (2018). Geohazard cascade and mechanism of large debris flows in Tianmo Gully, SE Tibetan Plateau and implications to hazard monitoring. *Eng. Geology* 233, 172–182. doi: 10.1016/j.enggeo.2017.12.013

Xie, S. B., Qu, J. J., Pang, Y. J., Zhang, K. C., and Wang, C. (2021). Dynamic mechanism of blown sand hazard formation at the Jieqiong section of the Lhasa–Shigatse railway. *Geomat. Nat. Haz. Risk* 12, 153–165. doi: 10.1080/19475705.2020.1863268

Yang, Z. Q., Wei, L., Liu, Y. Q., He, N., Zhang, J., and Xu, H. (2023a). Discussion on the relationship between debris flow provenance particle characteristics, gully slope, and debris flow types along the Karakoram Highway. *Sustainability* 15, 1–15. doi: 10.3390/su15075998

Yang, Z. Q., Zhao, X. G., Chen, M., Zhang, J., Yang, Y., Chen, W. T., et al. (2023b). Characteristics, dynamic analyses and hazard assessment of debris flows in Niumiangou Valley of Wenchuan County. *Appl. Sci.* 13, 1–13. doi: 10.3390/app13021161

Ye, T. J., Shu, T., Li, J. J., Zhao, P. H., and Wang, Y. (2022). Study on dynamic stability prediction model of slope in Eastern Tibet section of Sichuan–Tibet Highway. *Math. Prob. Eng.* 21, 674. doi: 10.1155/2022/4230674

Zeng, J. Z., Xie, J. F., Liu, R., Mo, F., and Yang, X. M. (2023). Research on glacier elevation variability in the Qilian Mountains of the Qinghai-Tibet Plateau based on topographic correction by pyramid registration. *Remote Sensing* 15, 1–20. doi: 10.3390/rs15010062

Zeng, Q., Yang, Z., Zhang, X., Shang, Y., and Zhang, L. (2007). Hazard model and countermeasure to super-large debris-flow in Parlung River – Case study of the section from Zamu Town to Guxiang Gully. *Chin. J. Geol. Hazard Control* 18, 27–33. doi: 10.3969/j.issn.1003-8035.2007.02.006

Zhang, M. F., Ren, Q. S., Wei, X. H., Wang, J. S., Yang, X. L., Jiang, Z. S., et al. (2011). Climate change, glacier melting and streamflow in the Niyang River Basin, Southeast Tibet, China. *Ecohydrology* 4, 288–298. doi: 10.1002/eco.206

Zhao, X., Yang, Z., Meng, X., Wang, S., Li, R., Xu, H., et al. (2023). Study on mechanism and verification of columnar penetration grouting of time-varying Newtonian fluids. *Processes* 11, 1–13. doi: 10.3390/pr11041151

Zhou, W., Tang, C., Van Asch, T. W. J., and Zhou, C. H. (2014). Rainfall-triggering response patterns of post-seismic debris flows in the Wenchuan earthquake area. *Nat. Hazards* 70, 1417–1435. doi: 10.1007/s11069-013-0883-8

Zou, Q., Cui, P., Zhou, G. G. D., Li, S. S., Tang, J. X., Li, S., et al. (2018). A new approach to assessing vulnerability of mountain highways subject to debris flows in China. *Prog. Phys. Geography* 42, 305–329. doi: 10.1177/0309133318770985